Kinetic Characterization of the Inactivation of UDP-GlcNAc Enolpyruvyl Transferase by (Z)-3-Fluorophosphoenolpyruvate: Evidence for Two Oxocarbenium Ion Intermediates in Enolpyruvyl Transfer Catalysis

Dennis H. Kim,[†,‡] Watson J. Lees,[†,‡] Terry M. Haley,[§] and Christopher T. Walsh*[,‡]

Contribution from the Department of Biological Chemistry and Molecular Pharmacology, Harvard Medical School, Boston, Massachusetts 02115, and the Structural Chemistry Department, Glaxo Research and Development, Greenford, Middlesex, United Kingdom UB6 0HE

Received September 19, 1994[⊗]

Abstract: UDP-GlcNAc enolpyruvyl transferase (MurZ) catalyzes the transfer of an enolpyruvyl moiety from phosphoenolpyruvate (PEP) to the 3-OH of UDP-GlcNAc in a reaction that constitutes the first committed step in bacterial peptidoglycan assembly. In a preliminary communication (Kim et al. *J. Am. Chem. Soc.* **1994**, *116*, 6478−6479) we reported the formation of two enzyme-associated fluoro analogs—a covalent phosphofluorolactyl-enzyme adduct, **3**, and a phosphofluorolactyl-UDP-GlcNAc tetrahedral adduct, **4**—of the corresponding normal reaction intermediates, **1** and **2**, during inactivation of MurZ by both (*E*)- and (*Z*)-3-fluorophosphoenolpyruvate (FPEP). In this paper we present a detailed study of the kinetics of formation, interconversion and decomposition of **3** and **4**. Kinetic analysis of the formation of **3** and **4** using enzymatically-synthesized [^{32}P](*Z*)-FPEP demonstrates that the formation of these adducts is consistent with the measured limiting rate constant for inactivation of MurZ by (*Z*)-FPEP (k_{inact} = 1.8 min^{-1}). The kinetics of formation suggest that **3** and **4** are formed by parallel pathways from the enzyme•UDP-GlcNAc•(*Z*)-FPEP ternary complex, with an initial 5-fold kinetic preference for the formation of **4** over **3**. Analysis of the inactivation reaction over a long time period suggests that **3** and **4** are nearly isoenergetic, reaching an equilibrium ratio of 1.2 (**3**:**4**) through a slow equilibration at the active site of MurZ, with rate constants for direct interconversion of 0.1 min^{-1}. Evidence from experiments following the washout of ^{32}P from **3** and **4** as well as data on the rate of deuterium incorporation from D_2O into **4** strongly suggest that the two analogs interconvert directly, without involving C−H bond cleavage and FPEP formation. The rate constant for the return of **3** and **4** to FPEP, a measure of the reversibility of (*Z*)-FPEP inhibition, was 0.004 min^{-1}, corresponding to a ratio of ~400:1 in favor of enzyme bound with **3** and **4** versus enzyme in ternary complex with (*Z*)-FPEP and UDP-GlcNAc. The relative retardation in rate of breakdown of **4** relative to the analogous normal reaction intermediate, **2**, is estimated to be $>10^6$, accounting for the observed enzyme inactivation. Comparison of the kinetic data with (*Z*)-FPEP with rapid-quench data for the normal reaction with PEP (Brown et al. *Biochemistry* **1994**, *33*, 10638−10645) supports a mechanism in which formation and decomposition of the reaction tetrahedral intermediate, **2** or **4** as well as interconversion between **2** or **4** and the corresponding enzyme adduct, **1** or **3**, involves oxocarbenium ion intermediates. The (*Z*)-FPEP data are suggestive of a branching mechanism for normal MurZ catalysis, in which the primary pathway of catalysis is through direct formation and breakdown of the tetrahedral intermediate, **2**.

The ubiquitous cellular constituent phosphoenolpyruvate (PEP) plays a central role in metabolic processes by virtue of its high-energy phosphate bond (ΔG = −14.8 kcal/mol). While most enzymatic reactions utilizing PEP as a substrate involve cleavage of the P−O bond (Scheme 1, route a), two types of reactions have been shown to involve attack at the electrophilic C-2 position of PEP with the unusual cleavage of the C−O bond of PEP[1] (Scheme 1, route b): (1) formation of an enol ether linkage through transfer of the enolpyruvyl moiety in PEP to a cosubstrate alcohol (Scheme 1, route b_1) and (2) carbon−carbon bond formation, possibly resulting from attack of a nucleophile at the C-2 position of PEP, with generation of a carbanion at the C-3 position that attacks an electrophilic carbon center (Scheme 1, route b_2).[2]

One of two known enzymes carrying out a b_1-type reaction in Scheme 1, UDP-GlcNAc enolpyruvyl transferase (MurZ) catalyzes the formation of enolpyruvyl-UDP-GlcNAc from UDP-GlcNAc and PEP (Scheme 2), a reaction that constitutes the first committed step in the assembly of the peptidoglycan layer of the bacterial cell wall. The enol ether product undergoes subsequent reduction by UDP-GlcNAc enolpyruvyl reductase, MurB, and the resulting UDP-*N*-acetyl muramic acid serves as the molecular scaffold on which the peptidyl component of the cell wall is constructed.[3] The antibiotic fosfomycin has been shown to exert its antibacterial activity through alkylation of Cys 115 of MurZ.[4−6] The other enolpyruvyl transferase, 5-enolpyruvyl-shikimate-3-phosphate (EPSP) synthase, catalyzes

[†] D.H.K. and W.J.L. contributed equally to the work in this paper.
[‡] Harvard Medical School.
[§] Glaxo Research and Development.
[⊗] Abstract published in *Advance ACS Abstracts*, January 15, 1995.

(1) Haslam, E. *Shikimic Acid: Metabolism and Metabolites;* John Wiley and Sons, Ltd.: England, 1993.

(2) (a) DeLeo, A. B.; Dayan, J.; Sprinson, D. B. *J. Biol. Chem.* **1973**, *248*, 2344−2353. (b) Hedstrom, L.; Abeles, R. *Biochem. Biophys. Res. Comm.* **1988**, *157*, 816−820. (c) Sheffer-Dee-Noor, S.; Belakhov, V.; Baasov, T. *Bioorg. Med. Chem. Lett.* **1993**, *3*, 1583−1588. (d) Baasov, T.; Sheffer-Dee-Noor, S.; Kohen, A.; Jakob, A.; Belakhov, V. *Eur. J. Biochem.* **1993**, *217*, 991−999.

(3) Park, J. T. In *Escherichia Coli and Salmonella Typhirium, Vol. 1*; Neidhardt, F. C., Ed.; American Society for Microbiology: Washington, DC, 1987; Chapter 42.

(4) Kahan, F. M.; Kahan, J. S.; Cassidy, P. J.; Kropp, H. *Ann. N. Y. Acad. Sci.* **1974**, *235*, 364−386.

(5) Wanke, C.; Amrhein, N. *Eur. J. Biochem.* **1993**, *218*, 861−870.

0002-7863/95/1517-1494$09.00/0

Scheme 1. Enzymatic C–O vs P–O Cleavage Routes on PEP

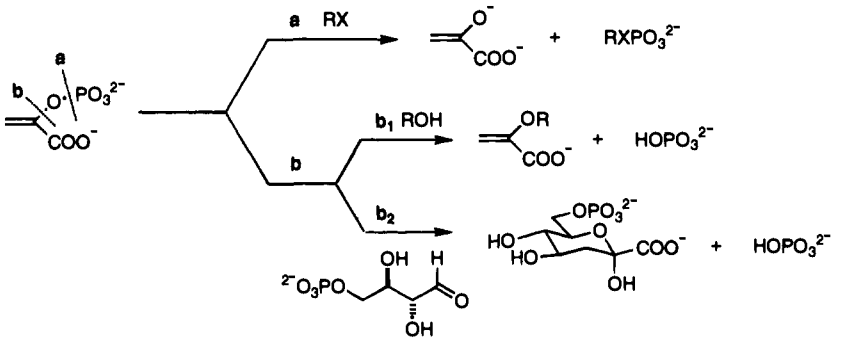

Scheme 2. The First Committed Step in Bacterial Peptidoglycan Assembly

PEP UDP-GlcNAc Enolpyruvyl UDP-GlcNAc

the sixth step in the shikimic acid pathway and is the site of action of the herbicide glyphosate.[7] MurZ and EPSP synthase share ~20% sequence identity,[8-10] and structural modeling based on this sequence homology and the crystal structure of EPSP synthase[11] suggests a similarity in overall fold, as well as alignment of putative active site residues.[12] A complete kinetic and thermodynamic characterization of the reaction pathway of EPSP synthase, performed by Anderson et al.,[13] unambiguously demonstrated the formation of a single tetrahedral intermediate from attack of the 5-OH group of shikimate-3-phosphate on C-2 of PEP. These data rigorously confirmed earlier proposals of the formation of this intermediate[14] and indicated that no covalent enzyme-PEP adduct is formed on the reaction pathway.

The cloning and overexpression of the *E. coli* and *E. cloacae* genes encoding UDP-GlcNAc enolpyruvyl transferase have greatly facilitated a mechanistic study of the enzyme.[8,9] Purification and characterization of MurZ has shown that the enzyme copurifies with 1 equiv of covalently-bound PEP.[5,15] Early studies had suggested that the reaction mechanism of MurZ involved a covalent adduct between enzyme and PEP,[16] but detailed insight into the nature of the reaction intermediates awaited the application of pre-steady-state kinetics measurements using rapid-quench techniques. These recent studies have led to the isolation and characterization of two kinetically competent reaction intermediates—a covalent phospholactyl-enzyme adduct, **1**, and a phospholactyl-UDP-GlcNAc tetrahedral intermediate, **2** (Scheme 3).[15,17]

Preliminary modeling has shown that the pre-steady-state kinetics data[15] are consistent with a sequential mechanism, in which formation of **1** precedes the formation of **2**. However, these data do not exclude the possibility of other mechanisms, such as a branching mechanism in which **2** would be formed by direct attack of the 3-OH of UDP-GlcNAc on C-2 of PEP, followed by rapid equilibration between **2** and **1**.

Although the formation of a covalent phospholactyl-enzyme adduct, **1**, is the major distinction between the mechanisms of catalysis by MurZ and EPSP synthase, the structural and functional homologies are suggestive of common mechanistic features, as evidenced by the isolation of **2** in the MurZ reaction[15,17] and the corresponding 5-phospholactyl-shikimate-3-phosphate tetrahedral adduct in the EPSP synthase reaction pathway.[13] The isolation and structural characterization of the reaction intermediates still leaves mechanistic questions related to the chemical steps of interconversion between substrates, intermediates, and products unanswered. Specific questions include the following: (1) Is addition to the C-2 position of PEP by cosubstrate alcohol concerted or stepwise with initial protonation at the C-3 position of PEP? (2) What is the mechanism of breakdown of the tetrahedral intermediate to enolpyruvyl product, and how does the enzyme abstract the nonacidic methyl hydrogen in **2** that is necessary for formation of the enol product?

In this paper we address these issues through the use of (*Z*)-3-fluorophosphoenolpyruvate ((*Z*)-FPEP) as a pseudosubstrate and mechanistic probe of MurZ. Fluorinated analogs of substrates have long been of interest as potential inhibitors of enzymes in view of the maximal electronegativity and steric compactness of the fluorine substituent.[18] In particular, (*E*)- and (*Z*)-FPEP have been synthesized and examined for their reactivity with several PEP-utilizing enzymes.[19,20] In a preliminary communication[21] we reported the inactivation of MurZ by both (*E*)- and (*Z*)-FPEP with the formation of two fluoro

(6) Marquardt, J. L.; Brown, E. D.; Lane, W. S.; Haley, T. M.; Ichikawa, Y.; Wong, C.-H.; Walsh, C. T. *Biochemistry* **1994**, 10646–10651.

(7) (a) Steinrucken, H. C.; Amrhein, N. *Biochem. Biophys. Res. Comm.* **1980**, *94*, 1207–1212. (b) Steinrucken, H. C.; Amrhein, N. *Eur. J. Biochem.* **1984**, *143*, 351–357.

(8) Wanke, C.; Falchetto, R.; Amrhein, N. *FEBS Lett.* **1992**, *301*, 271–276.

(9) Marquardt, J. L.; Siegele, D. A.; Kolter, R.; Walsh, C. T. *J. Bacteriol.* **1992**, *174*, 5748–5752.

(10) Duncan, K.; Lewendon, A.; Coggins, J. R. *FEBS Lett.* **1984**, *170*, 59–63.

(11) Stallings, W. C.; Abdel-Meguid, S. S.; Lim, L. W.; Shieh, H.-S.; Dayringer, H. E.; Leimgruber, N. K.; Stegeman, R. A.; Anderson, K. S.; Sikorski, J. A.; Padgette, S. R.; Kishore, G. M. *Proc. Natl. Acad. Sci. U.S.A.* **1991**, *88*, 5046–5050.

(12) Marquardt, J. L. Ph. D. Thesis, Department of Biological Chemistry and Molecular Pharmacology, Division of Medical Sciences, Harvard University, 1993.

(13) (a) Anderson, K. S.; Sikorski, J. A.; Johnson, K. A. *Biochemistry* **1988**, *27*, 7395–7406. (b) Anderson, K. S.; Sikorski, J. A.; Benesi, A. J.; Johnson, K. A. *J. Am. Chem. Soc.* **1988**, *110*, 6577–6579. (c) Anderson, K. S.; Johnson, K. A. *Chem. Rev.* **1990**, *90*, 1131–1149. (d) Anderson, K. S.; Johnson, K. A. *J. Biol. Chem.* **1990**, *265*, 5567–5572.

(14) Bondinell, W. E.; Vnek, J.; Knowles, P. F.; Sprecher, M.; Sprinson, D. B. *J. Biol. Chem.* **1971**, *246*, 6191–6196.

(15) Brown, E. D.; Marquardt, J. L.; Lee, J. P.; Walsh, C. T.; Anderson, K. S. *Biochemistry* **1994**, 33, 10638–10645.

(16) (a) Cassidy, P. J.; Kahan, F. M. *Biochemistry* **1973**, *12*, 1364–1374. (b) Zemell, R. I.; Anwar, R. A. *J. Biol. Chem.* **1975**, *250*, 4959–4964.

(17) Marquardt, J. L.; Brown, E. D.; Walsh, C. T.; Anderson, K. S. *J. Am. Chem. Soc.* **1993**, *115*, 10398–10399.

(18) (a) Walsh, C. T. *Adv. Enzymol. Relat. Areas Mol. Biol.* **1983**, *55*, 198–285. (b) Abeles, R. H.; Alston, T. A. *J. Biol. Chem.* **1990**, *265*, 16705–16708.

(19) Stubbe, J. A.; Kenyon, G. L. *Biochemistry* **1972**, *11*, 338–345.

(20) Duffy, T. H.; Nowak, T. *Biochemistry* **1984**, *23*, 661–670.

(21) Kim, D. H.; Lees, W. J.; Walsh, C. T. *J. Am. Chem. Soc.* **1994**, *116*, 6478–6479.

Scheme 3. Intermediates in the MurZ Reaction Pathway

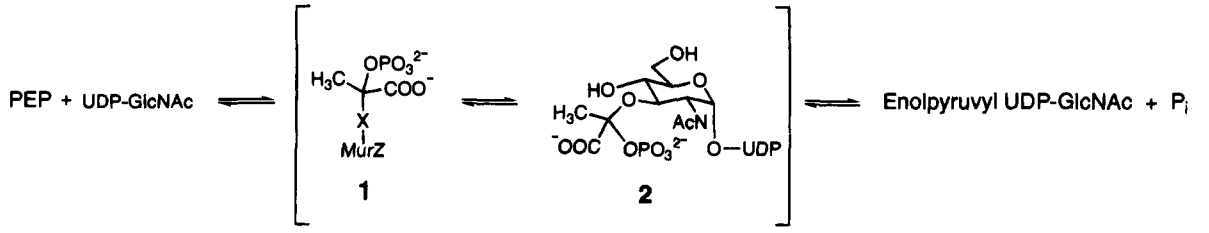

Scheme 4. Formation of Two Reaction Intermediate Analogs during Inactivation of MurZ by (*E*)- or (*Z*)-FPEP

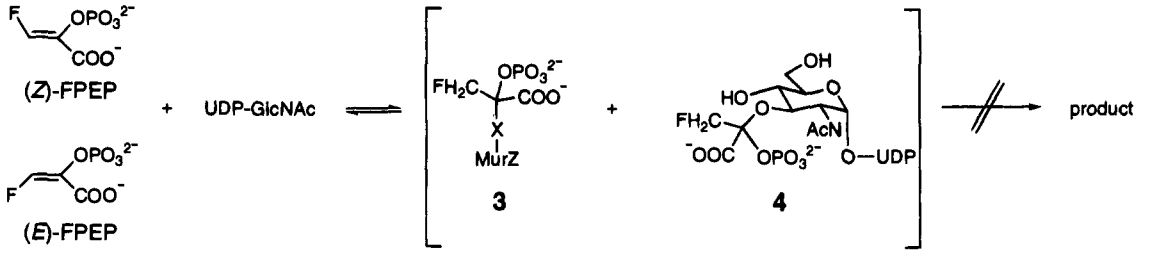

analogs, **3** and **4** (Scheme 4), of the normal intermediates, **1** and **2**. A previous study had demonstrated time-dependent inactivation of EPSP synthase by (*Z*)-FPEP, but not (*E*)-FPEP, through the accumulation of a comparable fluoro analog of the tetrahedral intermediate at the active site of that enzyme.[22] The modes of inactivation of MurZ and EPSP synthase by (*Z*)-FPEP appear to be similar—inability of a fluoromethyl analog of the tetrahedral intermediate to decompose in the forward direction. At the same time, the observation of **3**, in addition to **4**, at the MurZ active site underscores the primary mechanistic difference between the two enolpyruvyl transferases.

We have investigated the kinetics of processing of the fluorinated pseudosubstrate, (*Z*)-FPEP, by MurZ and present evidence for a branching mechanism for MurZ autoinactivation that involves direct formation of **4**, without requisite formation of **3**. Comparison of these data with the rapid-quench data for the MurZ reaction with PEP[15] reveal dramatic retardations in rate that can be attributed to the inductive effects of the fluoro substituent. Implications of these data on the reaction pathway of MurZ as well as the general enzymatic mechanism of enolpyruvyl transfer are discussed.

Experimental Section

Materials. (*E*)- and (*Z*)-FPEP were the generous gifts of Prof. Timor Baasov (Department of Chemistry, Technion—Israel Institute of Technology) and Prof. Ronald Somerville (Department of Biochemistry, Purdue University), respectively. Overexpression and purification of MurZ were performed as described previously.[9,15] Where specifically indicated, PEP-free MurZ was prepared and used as described previously.[15] Pyruvate phosphate dikinase (PPDK) was the generous gift of Dr. Linda Yankie and Prof. Debra Dunaway-Mariano (Department of Chemistry, University of Maryland).

Enzymatic Synthesis of Radiolabeled Compounds. [^{32}P](*Z*)-FPEP was synthesized by using 3-fluoropyruvate and [β-^{32}P]ATP as substrates for PPDK in the presence of inorganic pyrophosphatase, based on the previous observation that (*Z*)-FPEP, but not (*E*)-FPEP, served as a substrate for PPDK.[20] PPDK (100 units), inorganic pyrophosphatase (Sigma, 10 units), HEPES (pH 7.0, 50 mM), KH_2PO_4 (25 mM), $MgCl_2$ (5 mM), NH_4Cl (25 mM), 3-fluoropyruvate (Na^+ salt, 25 mM), ATP (1 mM) and [β-^{32}P]ATP (custom synthesis from ICN, 0.5 mCi, 900 Ci/mmol) were incubated in a volume of 500 μL for 2 h at 25 °C. The reaction mixture was centrifuged (13 000 × g, 10 min) through a membrane of molecular weight cutoff 30 000 (30 kDa filter, Amicon), and 10 U of Apyrase (Grade VII, Sigma) was added to the filtrate. Following a further 15 min incubation, [^{32}P](*Z*)-FPEP was purified from the filtrate by anion-exchange HPLC. (Anion-exchange HPLC was performed as described previously.[15]) The product of a duplicate reaction without labeled ATP was characterized by NMR, and the ^{32}P-labeled product was shown to co-elute with a sample of authentic material. [^{32}P]**4** was prepared by incubating MurZ (112 μM) with UDP-GlcNAc (1.3 mM) and [^{32}P](*Z*)-FPEP (80 μM, 400 mCi/mmol) in a volume of 960 μL for 4 min, followed by quenching of the reaction by the addition of 40 μL of 5 N KOH. The quenched reaction was passed through a 30 kDa filter, and [^{32}P]**4** was purified from the filtrate by anion-exchange HPLC. [^{32}P]**3** was prepared by incubating PEP-free MurZ (80 μM) with [^{32}P](*Z*)-FPEP (40 μM, 400 mCi/mmol) in a volume of 500 μL for 12 h at 4 °C. SDS-PAGE analysis indicated that ~10% of the [^{32}P](*Z*)-FPEP had been converted to the covalent enzyme-FPEP adduct, **3**. Excess [^{32}P](*Z*)-FPEP was partially removed (diluted 20-fold) by desalting the mixture by centrifuging the sample through a 30 kDa filter to a volume of 100 μL and resuspending in 50 mM Tris (pH 8.0) to a volume of 500 μL two times. [^{14}C]**2** was prepared by incubating MurZ (30 μM), [^{14}C]UDP-GlcNAc (30 μM, 309 mCi/mmol) (Amersham), 300 μM PEP, and 10 mM phosphate in a volume of 500 μL for 2 min, followed by quenching in 0.2 N KOH and purification by anion-exchange HPLC. [^{14}C]**4** was prepared by incubating PEP-free MurZ (30 μM), [^{14}C]UDP-GlcNAc (40 μM, 309 mCi/mmol), with (*Z*)-FPEP (500 μM) in a volume of 400 μL for 8 min, followed by quenching in 0.2 N KOH and purification by anion-exchange HPLC. Large-scale synthesis of unlabeled **4** was performed by incubating MurZ (0.8 mM) with UDP-GlcNAc (5 mM) and (*Z*)-FPEP (5 mM) in a volume of 1.7 mL for 5 min, followed by quenching of the reaction mixture in 0.2 N KOH, filtration through a 30 kDa filter, and purification of **4** from the filtrate by anion-exchange HPLC.

Methods. (*E*)- and (*Z*)-FPEP inactivation assays were performed at 25 °C by preincubating MurZ (5 μM), UDP-GlcNAc (0.5 mM), varying concentrations of (*E*)-FPEP (18, 25, 35, 50, and 100 μM) or (*Z*)-FPEP (30, 40, 60, 100, and 200 μM), and Tris buffer (50 mM, pH 8.0). At 10 s intervals, a 50 μL aliquot of the preincubation mix was diluted 1:20 and remaining MurZ activity was measured by a coupled assay utilizing MurB.[23] For each concentration of (*E*)- or (*Z*)-FPEP, an apparent first-order rate constant for inactivation (k_{app}) was obtained, and a plot of $1/k_{app}$ versus 1/[(*E*)- or (*Z*)-FPEP] yielded the values for k_{inact} and K_i.[24]

For kinetic experiments that followed the time course of [[^{32}P]**3**] and [[^{32}P]**4**], equal volumes were mixed at $t = 0$ to give the final concentrations indicated for each experiment, in a total volume that provided for 40 μL per time point. At indicated times, a 40 μL aliquot was quenched by addition to 40 μL of 0.4 N KOH, and 20 μL was

(22) Walker, M. C.; Jones, C. R.; Somerville, R. L.; Sikorski, J. A. *J. Am. Chem. Soc.* **1992**, *114*, 7601–7603.

(23) Benson, T. E.; Marquardt, J. L.; Marquardt, A. C.; Etzkorn, F. A.; Walsh, C. T. *Biochemistry* **1993**, *32*, 2024–2030.

(24) Morrison, J. F.; Walsh, C. T. *Adv. Enzymol. Relat. Areas Mol. Biol.* **1988**, 201–301.

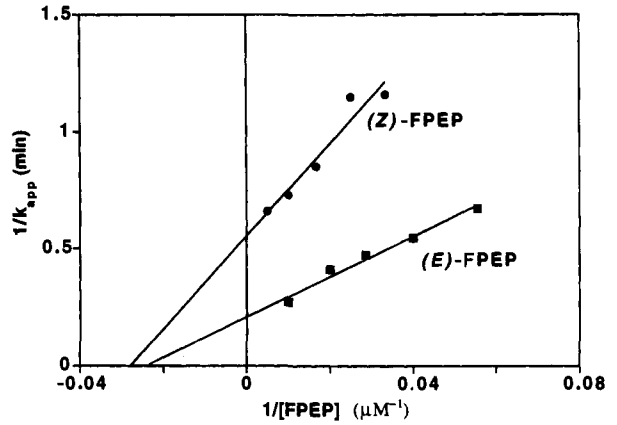

Figure 1. Determination of K_i and k_{inact} for (*E*)- and (*Z*)-FPEP. Pseudo-first-order rate constants for inactivation, k_{app}, were obtained for preincubation reactions consisting of MurZ (5 μM), UDP-GlcNAc (0.5 mM), and the following inhibitor concentrations: [(*E*)-FPEP] = 18, 25, 35, 50, 100 μM, and [(*Z*)-FPEP] = 30, 40, 60, 100, and 200 μM.

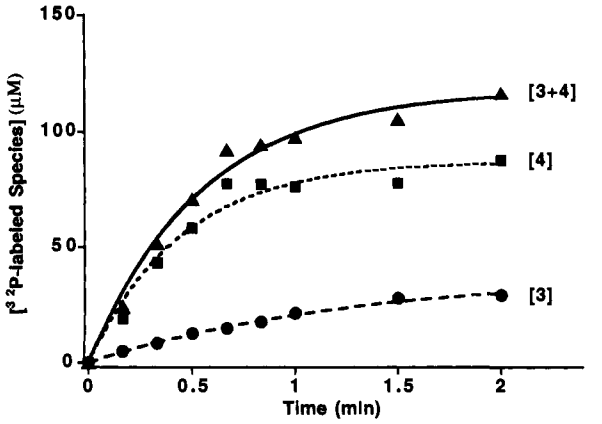

Figure 2. Determination of k_{inact} from direct measurement of the rate constant for formation of **3** + **4** using [^{32}P](*Z*)-FPEP. A reaction consisting of MurZ (100 μM), UDP-GlcNAc (1 mM), and [^{32}P](*Z*)-FPEP (350 μM) was quenched at 10, 20, 30, 40, 50, 60, 90, and 120 s, followed by HPLC and SDS-PAGE determination of radiolabeled [**3**] and [**4**].

subjected to SDS-PAGE, while the remaining 60 μL was centrifuged through a 30 kDa filter, and the filtrate was analyzed by anion-exchange HPLC. SDS-PAGE and quantitative autoradiography (Molecular Dynamics Phosphoimager, Sunnyvale, CA), and anion-exchange HPLC were performed for the quantitation of [**3**] and [**4**], as described previously for the analysis of **1** and **2**.[15] Curve-fitting of the data was performed using the Kaleidograph software program (Synergy Software, Reading, PA).

Nonenzymatic breakdown of **2** and **4** was examined by incubating [^{14}C]**2** or [^{14}C]**4** at pH 5.0 (100 mM NaAcetate) or pH 8.0 (50 mM Tris·HCl) and quenching aliquots at different times in 0.2 N KOH, followed by analysis by anion-exchange HPLC.

Results

Kinetics of MurZ Inactivation by FPEP. Time-dependent inhibition was observed upon preincubation of MurZ with (*E*)- or (*Z*)-FPEP in the presence of UDP-GlcNAc. For each concentration of (*E*)- or (*Z*)-FPEP used, a pseudo-first-order rate constant (k_{app}) was obtained, and limiting rate constants for inactivation (k_{inact}s) and K_is for (*E*)- and (*Z*)-FPEP were extracted from plots of $1/k_{app}$ vs 1/[(*E*)- or (*Z*)-FPEP] (Figure 1). For (*E*)-FPEP, K_i = 38 ± 16 μM; k_{inact} = 4.6 ± 1.1 min^{-1}. For (*Z*)-FPEP, K_i = 36 ± 19 μM; k_{inact} = 1.8 ± 0.4 min^{-1}.

In an earlier communication,[21] we reported the characterization, by NMR and mass spectrometry, of two reaction intermediate analogs—a covalent phosphofluorolactyl-enzyme adduct, **3**, and a phosphofluorolactyl-UDP-GlcNAc intermediate, **4**—that accumulated at the active site of MurZ during inactivation by (*E*)- or (*Z*)-FPEP. In this paper, we have directly measured the kinetics of formation of these two species, **3** and **4**, by using enzymatically-synthesized [^{32}P](*Z*)-FPEP. Figure 2 shows the data from a reaction containing MurZ, UDP-GlcNAc, and a saturating concentration of [^{32}P](*Z*)-FPEP (~10K_i) that was quenched at early (t < 2 min) time points. The time course of formation of **3** + **4** was fit to a single exponential function, from which a rate constant for accumulation of **3** + **4** of 1.8 min^{-1} was obtained. The initial velocities of formation of the two species, **3** and **4**, were compared by performing a linear fit to the rise of [**3**] and [**4**] (t < 40 s) in Figure 2, from which a ~5-fold kinetic preference for initial formation of **4** over **3** was measured. The amplitude of the exponential function fitting the rate of formation of **3** + **4** was 120 μM ([MurZ] = 100 μM), which is consistent, within experimental error, with a 1:1 stoichiometry of inactivation of MurZ by (*Z*)-FPEP.

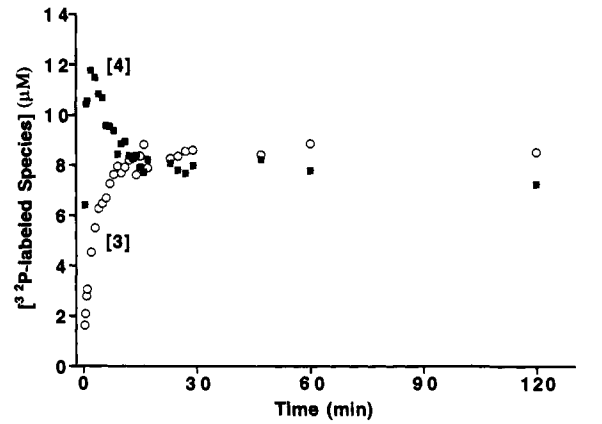

Figure 3. Time course of the formation of **3** and **4** during inactivation of MurZ by (*Z*)-FPEP. A reaction consisting of MurZ (50 μM), UDP-GlcNAc (0.5 mM), and [^{32}P](*Z*)-FPEP (17 μM) was quenched at the indicated times, followed by HPLC and SDS-PAGE determination of radiolabeled [**3**] and [**4**].

A reaction consisting of UDP-GlcNAc, [^{32}P](*Z*)-FPEP and MurZ in excess was also followed over a longer time period (Figure 3). All of the (*Z*)-FPEP was consumed within the first 2 min of the reaction, and over this initial time period, the major species formed was **4**, as observed in Figure 2. However, the initial rise in [**4**] was followed by a decrease over the following ~10 min, with a concomitant rise in [**3**], with the two species approaching an equilibrium ratio of **3**:**4** of approximately 1.2, even though the enzyme was nominally inactivated during this period as assessed by standard assay. The thermodynamic partitioning in slight favor of **3** is in clear contrast to the initial kinetic preference shown for the formation of **4**.

Figure 4a shows the results obtained from the addition of isolated [^{32}P]**4** back to an excess amount of MurZ, which show a decrease of [**4**] with a corresponding rise in [**3**] over a period of ~10 min with the two species again reaching the same equilibrium ratio of **3**:**4** of 1.2. Also shown on Figure 4a are exponential fits to the decay of **4** and the rise of **3**, both of which gave rate constants for approach to equilibrium of 0.2 min^{-1}. The amplitudes of the exponential fits corresponded to the observed equilibrium ratio of **3** to **4** of 1.2. Because the rate constant for the approach to equilibrium is the sum of the forward and backward rate constants for the interconversion between **3** and **4**, and given that the equilibrium ratio of **3** to **4** is 1.2:1.0, the rate constant for the formation of **4** from **3** can

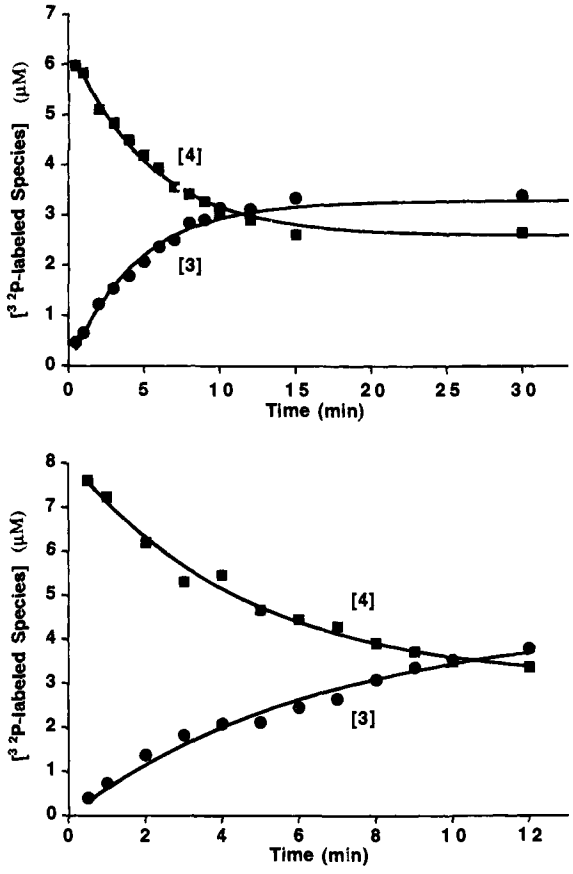

Figure 4. (a, top) Time course of the formation of **3** from isolated **4** and MurZ. [^{32}P]**4** was prepared as described in the Experimental Section. [^{32}P]**4** (9 μM) was added to MurZ (50 μM) and UDP-GlcNAc (0.5 mM), and the reaction was quenched at the indicated times, followed by HPLC and SDS-PAGE determination of radiolabeled [**3**] and [**4**]. (b, bottom) Same as in part (a), except unlabeled (*Z*)-FPEP (1 mM) was present in the reaction.

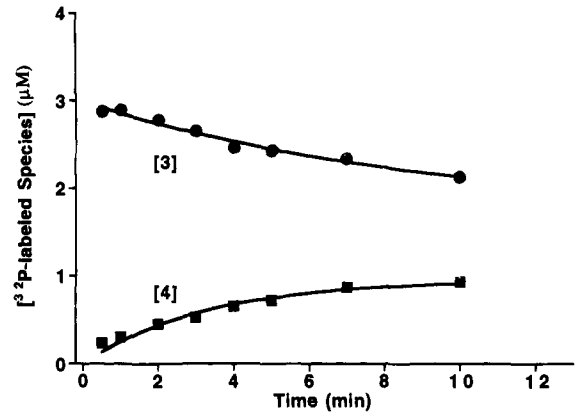

Figure 5. Time course of the formation of **4** from **3**. [^{32}P]**3** was prepared as described in the Experimental Section. At $t = 0$, UDP-GlcNAc (0.5 mM) and unlabeled (*Z*)-FPEP (1 mM) were added to [^{32}P]-**3** (3 μM), and the reaction was quenched at the times indicated on the plot, followed by HPLC and SDS-PAGE determination of radiolabeled [**3**] and [**4**].

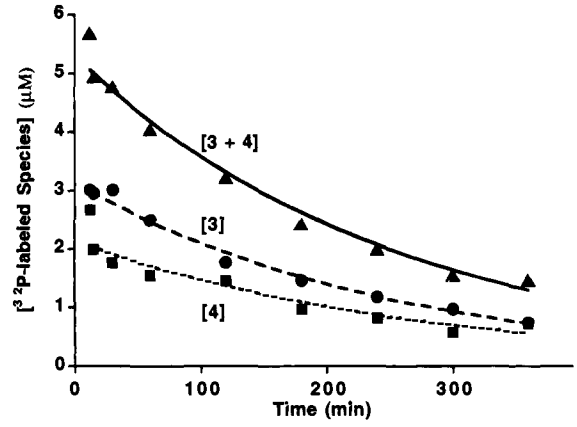

Figure 6. Time course of the washout of ^{32}P from **3** and **4**. [^{32}P]**4** was prepared as described in the Experimental Section. [^{32}P]**4** (9 μM) and unlabeled (*Z*)-FPEP (1 mM) were added to MurZ (50 μM) and UDP-GlcNAc (0.5 mM), and the reaction was quenched at the times indicated on the plot, followed by HPLC and SDS-PAGE determination of radiolabeled [**3**] and [**4**].

be deduced to be 0.09 min^{-1}, and the rate constant for the formation of **3** from **4** can be deduced to be 0.11 min^{-1}.

Figure 4b shows the results obtained from the addition of [^{32}P]**4** back to MurZ in the presence of a 100-fold excess of unlabeled (*Z*)-FPEP. Over the initial 10 min period shown, the data are equivalent to those shown in Figure 4a, with the rate constants for the approach of [**3**] and [**4**] to equilibrium both equal to 0.2 min^{-1}, giving the same forward and backward rate constants for the interconversion between **3** and **4** as derived from the data in Figure 4a. Only at longer times does washout of ^{32}P from **3** and **4** begin to be observed (see Figure 6).

The formation of **4** from **3** was followed by first preparing [^{32}P]**3** in the absence of UDP-GlcNAc as described in the Experimental Section. Figure 5 shows the time course of conversion of **3** to **4** following the addition of UDP-GlcNAc and excess unlabeled (*Z*)-FPEP (1 mM) to [^{32}P]**3**. The rate constant for the approach of **3** to equilibrium was fit as 0.1 min^{-1}, while the rate constant for the approach of **4** to equilibrium was fit as 0.3 min^{-1}. The equilibrium ratio of **3**:**4** was fit as 1.7:1.0. The deviation of the individual rate constants for the approach of species **3** and **4** to equilibrium (0.1 and 0.3 versus 0.2 min^{-1}) and the deviation of the equilibrium ratio (1.7 compared to 1.2) from the values observed in the experiments shown in Figures 3 and 4 most likely arises from the experimental difficulties in the preparation of [^{32}P]**3**. The conditions under which [^{32}P]**3** were prepared, involving a 12 h preincubation of MurZ with [^{32}P](*Z*)-FPEP, most certainly results in partial loss of enzyme activity. The population of inactive MurZ enzyme that still retains a covalently-attached ^{32}P label contributes a constant amount to the observed [**3**], potentially resulting in an overestimate of the equilibrium value.

The rate constant for return of **3** and **4** to FPEP was determined by two methods. In the first method (eq 1) [^{32}P]**4** was added to MurZ, and following the equilibration between **3**

$$E + 4^{*} \xrightarrow[\text{fast}]{} E{\cdot}4^{*} \xrightarrow[0.2\ min^{-1}]{} E{\cdot}\{3^{*} + 4^{*}\} \xrightarrow[\text{slow}]{} E{\cdot}U{\cdot}FPEP^{*} \xrightleftharpoons[\text{fast}]{} E{\cdot}U + FPEP^{*} \quad (1)$$

E, MurZ; U, UDP-GlcNAc; * denotes ^{32}P-labeled species;

and **4** over ~10 min, the washout of the ^{32}P label out of **3** and **4** in the presence of excess unlabeled (*Z*)-FPEP was observed over 5 h (Figure 6). As expected, the rate constants for washout of ^{32}P from **3** and **4** are comparable, and a fit to the data gave a rate constant for the washout of ^{32}P from **3** + **4** of 0.004 min^{-1}. In the second method (eq 2), isolated perprotio-**4** was added to MurZ in D_2O, and ^{19}F-NMR of **4** from quenched aliquots of the incubation was used to follow deuterium incorporation into **4** over time (Figure 7). The triplet corresponding to perprotio-**4** was centered at −224.8 ppm, while the doublet corresponding to the monodeutero-**4** species was centered at −225.5 ppm. The spectra from reaction aliquots quenched at $t = 60$ and 165 min show the gradual decrease in

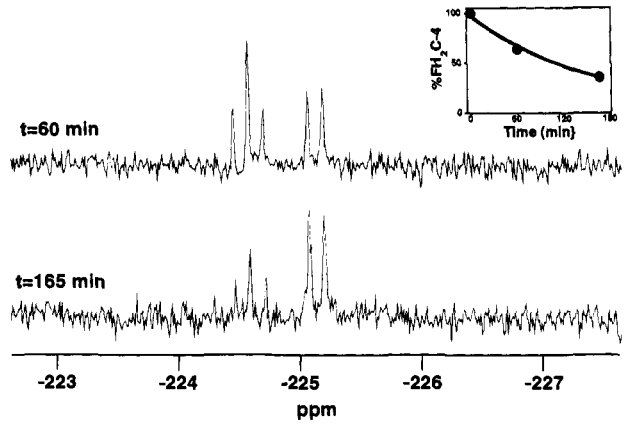

Figure 7. Time course of D_2O exchange into **4** followed by ^{19}F-NMR spectroscopy, as described in eq (2). Perprotio-**4** (~400 μg, 0.25 mM) was added to 90 mg MurZ (1 mM) and UDP-GlcNAc (2 mM) in D_2O, and the reaction was quenched in 0.2 N KOH after 60 and 165 min. Inset shows a plot of the amount of remaining perprotio-**4** as a percentage of total **4** species vs time. ^{19}F-NMR spectra were recorded for 2 h on a Bruker AM400 spectrometer operating at a frequency of 376 MHz. Spectra were referenced to an external standard of 1% TFA ($\delta = -76.53$ ppm).

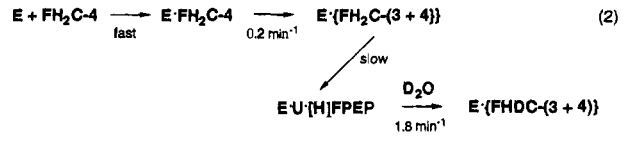

(2)

E, MurZ; U, UDP-GlcNAc; [H]FPEP, protio-FPEP;

FH_2C-, perprotio species; FHDC-, monodeutero species;

the triplet and concomitant increase in the doublet, and a fit to a plot of % perprotio-**4** vs time (Figure 7, inset) gave a rate constant for the formation of FPEP from **3** + **4** of 0.006 min^{-1}. (The spectrum of an aliquot taken after 13 h (data not shown) shows the complete disappearance of the triplet, with the appearance of a singlet peak, centered at −226 ppm, arising from perdeutero-**4**. Assuming stereospecific addition of D^+ to C-3 of (*E*)- or (*Z*)-FPEP, the formation of perdeutero-**4** is strongly suggestive of free rotation of the fluoromethyl group of **4** in the active site of MurZ.)

The kinetic data for the MurZ reaction with (*Z*)-FPEP are summarized in Table 1, along with the corresponding data for the reaction with PEP[15] for comparison.

Nonenzymatic Decomposition of 2 and 4. Decomposition of **2** and **4** in solution was measured at pH 8.0 in the absence of enzyme. **2** decomposes, as expected for a ketal, primarily to UDP-GlcNAc, pyruvate, and phosphate with a rate constant of 5.4×10^{-3} min^{-1}. Less than 5% decomposition of **4** was observed over 50 h. Because the stability of **4** at pH 8.0 does not allow for quantitative comparison of the stabilities of **2** and **4**, decomposition at pH 5.0 was also followed. **2** was observed to decompose primarily to UDP-GlcNAc, pyruvate, and phosphate with a rate constant of 1.1 min^{-1}. The rate constant for decomposition of **4** to UDP-GlcNAc, 3-fluoropyruvate, and phosphate was measured to be 1.8×10^{-4} min^{-1} at pH 5.0. These data at pH 5.0 correspond to a relative retardation in rate constant of 6×10^3 effected by the fluoro substituent.

Discussion

Mechanism of Inactivation of MurZ by FPEP. The results in this paper and in our earlier communication[21] establish that both (*E*)- and (*Z*)-isomers of FPEP are pseudosubstrates for

Table 1. Comparison of Rate Constants for the Reaction of MurZ with PEP[15] and (*Z*)-FPEP

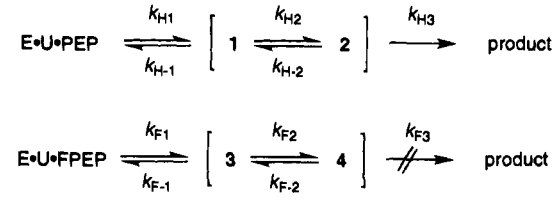

rate constant	k_H (min^{-1})	k_F (min^{-1})	k_H/k_F
k_1	2.43×10^4	1.8	10^4
k_{-1}		0.004	
k_2	10^2-10^5	0.09	10^3-10^6
k_{-2}	10^2-10^5	0.11	10^3-10^6
k_3	170	$<10^{-4}$	$>10^6$

MurZ, undergoing enzyme-mediated conversion to fluorinated analogs of normal reaction intermediates. These analogs, **3** and **4**, do not decompose detectably in the forward direction to form products, remaining tightly bound and stoichiometrically titrating the enzyme active sites, accounting for the observed inactivation. The recent precedent with EPSP synthase undergoing autoinactivation with (*Z*)-FPEP by accumulation of a tetrahedral phosphofluorolactyl intermediate[22] had led us to anticipate a similar formation of the analogous addition product of cosubstrate alcohol to C-2 of PEP, in this case, species **4**. More surprising was the formation of a covalent phosphofluorolactyl enzyme intermediate, **3**, in addition to **4**, in inactivated populations of MurZ. The observation of **3** and **4** during FPEP-inactivation of MurZ both reinforced the previous detection of **1** and **2** in normal catalytic turnover of PEP by the enzyme[15,17] and provided us with the opportunity to give further mechanistic definition to the reaction of MurZ with both PEP and FPEP through an investigation of the kinetics of FPEP inactivation.

Kinetic analysis of the pseudo-first-order inactivation of MurZ by (*E*)- and (*Z*)-FPEP is presented in Figure 1. Both (*E*)- and (*Z*)-FPEP inactivate MurZ with equivalent values of K_i, but there is a 2.5-fold kinetic preference for the (*E*)-isomer. This is in contrast to the preference for (*Z*)-FPEP in most PEP-utilizing enzymes[20] and, in particular, the stereospecificity of EPSP synthase for the (*Z*)- isomer.[22] Prolonged photoisomerization of (*Z*)-FPEP to an (*E*)/(*Z*)-FPEP mixture has been found to result in a 30:70 ratio of (*E*)-FPEP:(*Z*)-FPEP,[20] which is suggestive of greater thermodynamic stability of (*Z*)-FPEP relative to the (*E*)-isomer. The enhanced reactivity of the (*E*)-isomer with MurZ may result from a corresponding decrease in the activation energy required for formation of **3** and **4**.

Kinetic studies utilizing enzymatically-synthesized [^{32}P](*Z*)-FPEP were limited to the (*Z*)-isomer because of the stereospecificity of PPDK for the (*Z*)-FPEP product.[20] Kinetics of (*Z*)-FPEP reactivity with MurZ (Figure 2) yielded a rate constant for the formation of **3** + **4** of 1.8 min^{-1} at saturating [(*Z*)-FPEP], in agreement with the limiting rate constant for inactivation by (*Z*)-FPEP determined in Figure 1. The agreement in these two rate constants demonstrates that **3** and **4** are "kinetically-competent"; that is, the kinetics of accumulation of these species are consistent with the observed macroscopic kinetics of enzyme inactivation. The ~1:1 stoichiometry for inactivation observed also provides additional corroborative evidence that the observed inactivation of MurZ activity is due to the accumulation of **3** and **4**.

In addition, the initial rate constant for formation of **4** was greater than the initial rate constant for formation of **3** by a factor of 5; however, at long time points, as indicated in Figure

Scheme 5. Mechanism for Observed Direct Interconversion between 3 and 4

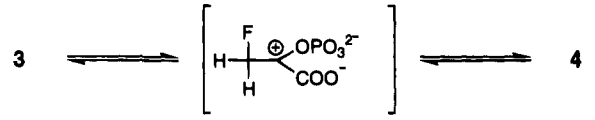

Scheme 6. Stepwise Mechanism for Attack on (Z)-FPEP

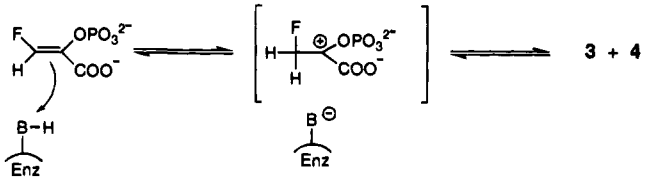

3, the ratio of 3 to 4 approaches 1.2. These data demonstrate the formation of 4 directly from the MurZ·UDP-GlcNAc·(Z)-FPEP (E·U·FPEP) ternary complex, without going through intermediate 3. In fact, the primary pathway of formation of 3 from E·U·FPEP appears to be through 4, although the initial linear rate of formation of 3 in Figure 2 suggests that there is also direct formation of 3 from the E·U·FPEP ternary complex.

The observation of approximately equivalent amounts of 3 and 4 at long time points represents an equilibration between 3 and 4 in the active site of the enzyme. The equilibrium was approached from both sides, starting with 4 (Figure 4a,b) as well as starting with 3 (Figure 5). From the value of the equilibrium between 3 and 4 and the determination of the rate constants for approach to equilibrium, the rate constants for the interconversion between 3 and 4 were deduced to be 0.11 min^{-1} for the formation of 3 from 4, and 0.09 min^{-1} for the formation of 4 from 3. The rate constants for interconversion between ^{32}P-labeled 3 and 4 were unaffected by the presence of unlabeled (Z)-FPEP in the reaction, consistent with the direct interconversion between 3 and 4, without intermediate formation of FPEP. A plausible mechanism for the direct interconversion between 3 and 4 involves an oxocarbenium ion intermediate (Scheme 5).

The reversibility of FPEP inactivation of MurZ was examined by determination of the rate constant for return to the E·U·FPEP ternary complex from 3 and 4. The rate constant for washout of ^{32}P from 3 and 4 (Figure 6) was determined to be 0.004 min^{-1}, in agreement with the estimated rate constant of 0.006 min^{-1} for deuterium incorporation into 4. Taken together with the limiting rate constant of inactivation, the determination of the rate constant for the reverse formation of the E·U·FPEP ternary complex from 3 and 4 gives a ratio of greater than 400:1 (1.8 min^{-1}/0.004 min^{-1}) in favor of enzyme bound with 3 and 4 versus enzyme in ternary complex with (Z)-FPEP and UDP-GlcNAc. In addition, the rate constant for formation of FPEP from 3 and 4 is ~20-fold slower than the rate constants for the interconversion between 3 and 4, confirming that interconversion between 3 and 4 does not proceed with C−H cleavage and E·U·FPEP formation. Deprotonation of the C-3 position of an oxocarbenium ion (Scheme 5) by an active site base and subsequent formation of FPEP may proceed with a rate constant that is ~1/20 the rate constant for capture of the electrophilic C-2 center of the oxocarbenium ion by either an active site nucleophile (most likely the thiolate side chain of Cys 115)[15] or the 3-OH of UDP-GlcNAc in a three-way competition at the active site of MurZ.

Effect of the Fluoro Substituent. Substitution of either vinylic hydrogen of PEP by fluorine has dramatic consequences on rates of intermediate formation, equilibration, and decay which can be interpreted in terms of the effect of the intense

Scheme 7. Stepwise (E1) Elimination Mechanism for Breakdown of the Phospholactyl-UDP-GlcNAc Tetrahedral Intermediate

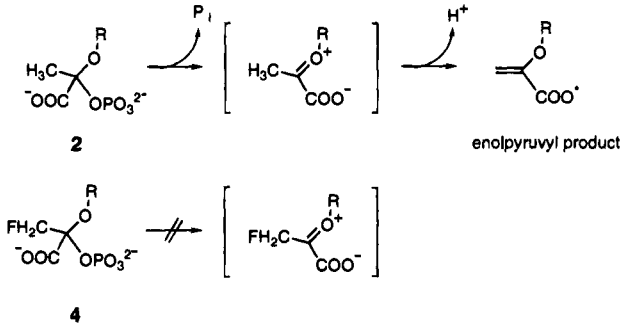

electronegativity of fluorine. Table 1 summarizes the rate constants for the formation, interconversion, and decomposition of 3 and 4 and compares these data to the rate constants derived from preliminary modeling of rapid-quench kinetics data of the normal reaction involving PEP.[15] The rate constant for formation of analogs 3 and 4 is slowed by a factor of 10^4 relative to the rate constant for formation of the normal tetrahedral intermediate, 2. The retardation in rate constant for formation is consistent with the mechanism in Scheme 6, in which the initial step of the reaction involves protonation at the C-3 position of (Z)-FPEP, generating an oxocarbenium ion intermediate that is destabilized by the presence of the fluoro substituent.

The values for the rate constants for interconversion between 1 and 2 in normal catalysis are dependent on the reaction mechanism on which modeling of rapid-quench data is based. A sequential mechanism, involving formation of 1 followed by 2, requires an extremely rapid pre-equilibrium, corresponding to rate constants of ~10^5 min^{-1} for the interconversion between 1 and 2. The previously published data[15] can also be fit satisfactorily to a branching mechanism (eq 3), with rate constants for the interconversion between 1 and 2 in the range

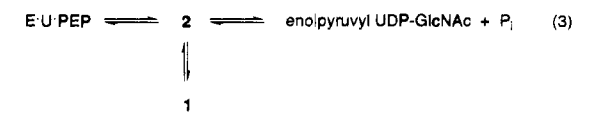

(3)

of ~10^2−10^5 min^{-1}. Comparison of the rate constants for interconversion between 3 and 4 to either set of rate constants for the interconversion between 1 and 2 demonstrate a significant rate retardation upon substitution of fluorine for hydrogen, on the order of 10^3−10^6. The dramatic retardation in rate constants for interconversion between 3 and 4 as compared to those for 1 and 2 is consistent with the mechanism in Scheme 5, in which the oxocarbenium ion intermediate is destabilized by the fluoro substituent.

Particularly striking and manifest in the macroscopic enzyme inactivation is the inability of 4 to breakdown in the forward direction toward product, indicating a high energy barrier to proton abstraction from the fluoromethyl group of 4. Scheme 7 shows a stepwise (E1) mechanism for the breakdown of 2 in the forward direction that is consistent with the observed greater than 10^6 retardation in rate constant for forward decomposition of 4.[21] In this mechanism, the lone pair of the ether oxygen assists in elimination of phosphate with cleavage of the C−O bond, generating another oxocarbenium ion intermediate and increasing the acidity of the adjacent C-3 methyl hydrogens for abstraction as a proton, charge quenching, and vinyl ether formation. The presence of a fluorine substituent at the C-3 position in 4 effects an insurmountable destabilization of the oxocarbenium ion transition state. In contrast, an E2-type mechanism for decomposition of 2, in which deprotonation at

Scheme 8. Proposed Mechanism of Catalysis by MurZ

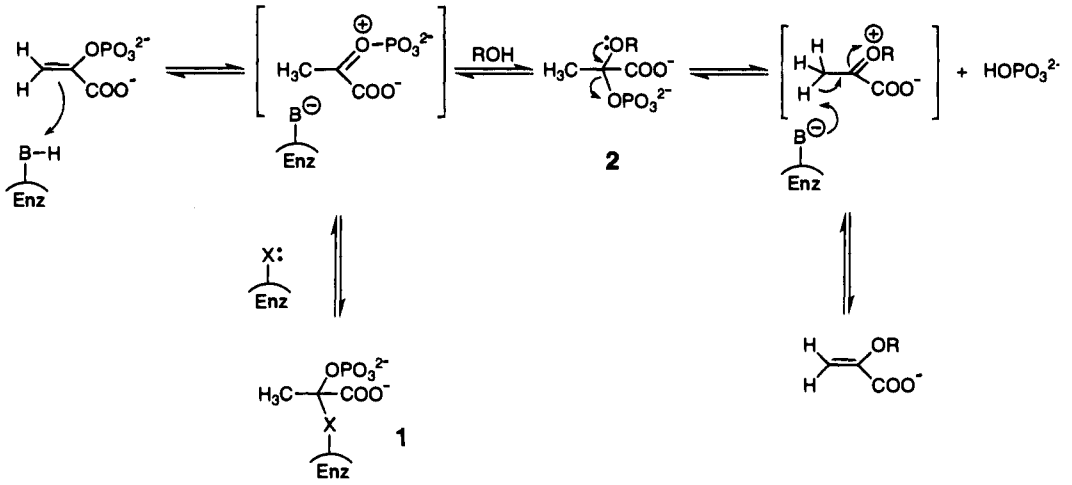

C-3 and elimination of phosphate occur in concert, would not be expected to be greatly affected by the substitution of fluorine at the C-3 position; in fact, the fluoro substituent might be predicted to increase the acidity of the C-3 hydrogen, with no expected retardation in rate of breakdown of **4**. Bartlett and co-workers have suggested that breakdown of the tetrahedral intermediate of the EPSP synthase reaction may proceed through an oxocarbenium ion, based on the synthesis of a difluoromethyl analog of the tetrahedral intermediate that is a potent inhibitor of EPSP synthase and unable to undergo enzyme-catalyzed breakdown to product.[25] Furthermore, Walker et al. found that the monofluoro analog of the tetrahedral intermediate accumulated at the active site during inactivation of EPSP synthase by (Z)-FPEP, with no observed breakdown to form an EPSP-like product.[22]

Increased stability of **4**, relative to **2**, to nonenzymatic breakdown is also suggestive that the lack of enzyme-catalyzed breakdown of **4** in the forward direction results from destabilization of the proposed oxocarbenium ion. Nonenzymatic breakdown, albeit primarily to different products—UDP-GlcNAc, 3-fluoropyruvate, and phosphate—than in enzyme-mediated breakdown may proceed through capture of an oxocarbenium ion by water. Such a mechanism of breakdown in solution has been proposed for the tetrahedral intermediate in the reaction catalyzed by EPSP synthase,[13] and fluoro analogs of the intermediate also show a similar dramatic stabilization to breakdown.[22,25]

There are other enzymatic cases in which dramatic rate reductions in reactions with fluorinated substrates have been interpreted in terms of inductive effects that destabilize carbocation intermediates. In particular, elegant studies by Poulter and co-workers[26] on the prenyl transfer reaction catalyzed by farnesyl pyrophosphate synthetase with fluorinated substrate analogs provided compelling evidence for a stepwise "ionization−condensation−elimination" mechanism involving transient formation of an allylic cation. A greater than 10^3-fold depression in the rate of prenyl transfer was observed with 2-fluorogeranyl pyrophosphate as a substrate analog.

Implications on the Mechanism of Enolpyruvyl Transfer Catalysis. On the basis of the data in this paper on the kinetics of processing of the pseudosubstrate (Z)-FPEP by MurZ and a consideration of the expected inductive effects of fluorine on the rates of formation, interconversion, and decay of intermediates (summarized in Table 1), we propose a detailed reaction mechanism for the MurZ reaction in Scheme 8, which addresses the following issues underlying the general mechanism of enolpyruvyl transfer catalysis.

First, protonation at C-3 of PEP precedes addition of cosubstrate alcohol to the C-2 position. Previous studies of EPSP synthase in which hydrogen exchange at the C-3 position of PEP in the presence of 4,5-dideoxy-shikimate-3-phosphate was observed were interpreted in terms of either the addition of an enzyme nucleophile at C-2 of PEP or transient formation of an oxocarbenium ion species.[27] The lack of identification of a covalent EPSP synthase-PEP adduct makes the former highly unlikely.[13] In the present work, we interpret the ~10^4-fold retardation in rate constant for formation of **4** from (Z)-FPEP relative to the rate constant for formation of **2** from PEP as being strongly suggestive of an initial protonation step, as the presence of the fluoro substituent would be expected to destabilize the formation of the oxocarbenium ion, giving the observed rate depression. The formation of this oxocarbenium ion is also implicated in the direct interconversion between **3** and **4**.

Second, breakdown of **2** in the forward direction is stepwise, proceeding through an oxocarbenium ion intermediate. The similar behavior of the fluorinated analogs of the tetrahedral intermediates for both the MurZ and EPSP synthase reactions, with respect to the mode of enzyme inactivation and stability to nonenzymatic breakdown, strongly implicate an oxocarbenium ion transition state in a common mechanism of breakdown of the respective reaction tetrahedral intermediates. Such a mechanism also accounts for the observed abstraction of a proton from the methyl group of the tetrahedral intermediate in forward breakdown. Without activation through an oxocarbenium ion, the p*K*a of the methyl proton would be expected to be large.

Finally, the kinetic data on the formation of **4** clearly demonstrate that its formation does not require prior formation of **3**. Extending this observation to normal catalysis involving the intermediates, **1** and **2**, we propose that the MurZ reaction pathway involves a branching mechanism, as depicted in Scheme 8, with the primary pathway for catalysis involving direct formation and breakdown of **2**. In this mechanism, the formation of **1** is the result of a readily-reversible adventitious

(25) (a) Alberg, D. G.; Lauhon, C. T.; Nyfeler, R.; Faasler, A.; Bartlett, P. A. *J. Am. Chem. Soc.* **1992**, *114*, 3535−3546. (b) Seto, C. T.; Bartlett, P. A. *J. Org. Chem.* **1994**, *59*, 7130−7132.

(26) (a) Poulter, C. D.; Argyle, J. C.; Mash, E. A. *J. Am. Chem. Soc.* **1977**, *99*, 957−959. (b) Poulter, C. D.; Argyle, J. C.; Mash, E. A. *J. Biol. Chem.* **1978**, *253*, 7227−7233. (c) Poulter, C. D.; Rilling, H. C. *Acc. Chem. Res.* **1978**, *11*, 307−313.

(27) Anton, D. L; Hedstrom, L.; Fish, S. F.; Abeles, R. H. *Biochemistry* **1983**, *22*, 5903−5908.

capture of the first oxocarbenium ion by an enzyme nucleophile, probably Cys 115.[5,6,15] Site-directed mutagenesis studies of Cys 115 suggest that this residue is essential for catalysis.[5,15] If formation of **1** is not required on the primary pathway for catalysis, as depicted in Scheme 8, we suggest that the essential role of Cys 115 is as an active site base participating in the initial C-3 protonation of PEP, with the thiolate side chain also playing a role in electrostatic stabilization of the proposed oxocarbenium ion intermediates. The lack of an analogous cysteine in EPSP synthase may preclude the reversible capture of the first oxocarbenium ion to form a covalent enzyme adduct. Further structural and mutagenesis studies should help elucidate the role of Cys 115 and identify additional critical residues involved in MurZ catalysis.

Acknowledgment. We thank Prof. Timor Baasov (Technion—Israel Institute of Technology) for insightful discussions on mechanism. We also thank Prof. Baasov and Prof. Ronald Somerville (Purdue University), for their gifts of (*E*)- and (*Z*)-FPEP, respectively, and Prof. Debra Dunaway-Mariano and Dr. Linda Yankie (University of Maryland) for their gift of pyruvate phosphate dikinase. We thank members of the Walsh group for comments on the manuscript. D.H.K. was supported by a Medical Scientist Training Program grant from the National Institutes of Health. W.J.L. was supported by a postdoctoral fellowship from the Natural Sciences and Engineering Research Council of Canada. This work was supported in part by National Institutes of Health Grant GM49338-01.

JA943102W